Florence, Italy 12-16 July 2015
ICSV22
The 22nd International Congress on Sound and Vibration

NUMERICAL STUDY OF THE ACOUSTIC RESPONSE OF A SINGLE ORIFICE WITH TURBULENT MEAN FLOW

Jonathan Tournadre and Paula Martínez-Lera
Siemens Industry Software, Researchpark 1237, Interleuvenlaan 68, 3001 Leuven, Belgium
email: jonathan.tournadre@siemens.com

Wim Desmet
KU Leuven, Dept. of Mechanical Engineering, Celestijnenlaan 300B, 3001 Leuven, Belgium

This paper investigates the effect of turbulent flow on the acoustic behavior of a single orifice through numerical simulations. Two different versions of the perturbed compressible linearized Navier-Stokes (LNS) equations, described in literature, are compared through computations based on a high-order finite element method. The first version considers the standard double decomposition of the field variables into steady fluid motion and harmonic perturbation. The second one is based on a triple decomposition that also distinguishes the contribution of turbulence to the fluctuation of the instantaneous field variables. This model requires a closure model for the introduced stress tensor interpreted as the oscillation of the background Reynolds stresses due to the periodic waves, which can be incorporated in the linearized equations through an eddy-viscosity model. The turbulent viscosity as well as the base flow properties are obtained from a two-equation Reynolds averaged Navier-Stokes (RANS) simulation. A detailed study on the modeling parameters is carried out at different Strouhal numbers.

1. Introduction

Acoustic liners and orifice structures are extensively applied in industry to suppress noise. In traditional applications, an acoustic liner absorbs noise passively and its damping performance depends on the characteristics of both the acoustic excitation and of the mean flow. Therefore accurate prediction methods are needed for prediction purposes as well as a thorough understanding of the system's acoustical properties linked to the flow conditions.

The main contributions to sound attenuation in laminar flow configurations come from visco-thermal effects, mean flow convection and interaction with entropic and vorticity modes. When sound waves propagate within turbulent flow, turbulent mixing can result in extra acoustic attenuation due to energy loss by turbulent absorption. This absorbing mechanism can be attributed to the turbulent stress acting on the sound wave. The purpose of the current work is to investigate the mechanisms of sound-flow and sound-turbulence interactions in low Mach number flow orifice configuration by means of numerical simulations. Two different versions of the perturbed compressible linearized Navier-Stokes (LNS) equations are employed here.

A comparison between triple (turbulent) and double (quasi-laminar) decomposed set of equations has been made in [1] on the case of a T-junction for Strouhal St number from 0 to 4. It has been

observed that for small Strouhal numbers $St < 0.5$ the behavior tends to a quasi-stationary response, with turbulent and quasi-laminar perturbed LNS giving similar results on the scattering matrix for a T-joint geometry, whereas it exists a frequency range where flow turbulence affects the acoustic wave propagation. The idea of this paper is to investigate if such conclusions are the same in case of an orifice under bias flow condition with a normal acoustic excitation. Such a configuration as already been successfully studied [2] with a standard Linearized Navier-Stokes equations Finite Element Method (FEM) solver in frequency domain, where the method has proved to successfully predict the whistling potential of such orifices. The aim of this paper is to assess the impact of flow and flow turbulence on the acoustic behavior of the orifice with a frequency domain LNS high-order FEM solver.

This paper describes the governing equations in Section 2 and the applied numerical technique in Section 3. Details on the base flow and harmonic perturbations numerical setup are given in Section 4 before presenting the results from the two versions of the perturbed LNS equations.

2. The Linearized Navier-Stokes equations

The linear regime of an orifice can be simulated by the perturbed version of the full compressible Navier-Stokes equations. In this section, we briefly discuss two approaches that differ in terms of the flow turbulence contribution to the perturbation field.

2.1 Quasi-laminar LNS equations

The traditional approach is to consider any instantaneous variable $q(\mathbf{x},t)$ as the sum of a variable describing the steady fluid motion $\bar{q}(\mathbf{x})$ and a relatively smaller harmonic perturbation $\tilde{q}(\mathbf{x},t)$. Assuming an isentropic flow and applying such variable decomposition, the linearized Navier-Stokes equations can be written as:

$$\begin{cases} \bar{\rho}\dfrac{\partial \tilde{u}_s}{\partial t} + \dfrac{\partial \bar{u}_r \bar{\rho}\tilde{u}_s}{\partial x_r} + \left(\bar{\rho}\tilde{u}_r + \tilde{\rho}\bar{u}_r\right)\dfrac{\partial \bar{u}_s}{\partial x_r} + \bar{c}^2\dfrac{\partial \tilde{\rho}}{\partial x_s} - \dfrac{\partial \tilde{\tau}_{sr}}{\partial x_r} = 0, & \text{(1a)} \\ \dfrac{\partial \tilde{\rho}}{\partial t} + \dfrac{\partial(\bar{\rho}\tilde{u}_r + \tilde{\rho}\bar{u}_r)}{\partial x_r} = 0, \qquad \text{with } \tilde{\tau}_{sr} = \mu\left(\dfrac{\partial \tilde{u}_s}{\partial x_r} + \dfrac{\partial \tilde{u}_r}{\partial x_s} - \dfrac{2}{3}\dfrac{\partial \tilde{u}_k}{\partial x_k}\delta_{rs}\right). & \text{(1b)} \end{cases}$$

where ρ, $\mathbf{u}$ and p are the density, velocity and pressure fields. μ is the dynamic fluid viscosity, δ the Kronecker delta function and τ_{sr} is the viscous stress tensor. In absence of temperature gradient in the investigated case, the fluid viscosity is assumed homogeneous over the entire domain. The set of equations Eq. (1) can be written in a more compact way using a matrix formulation to define a LNS equations operator $\mathcal{L}_{\mathcal{LNSE}}$:

$$\mathcal{L}_{\mathcal{LNSE}}(\mathbf{q}) = 0 \Leftrightarrow \frac{\partial \mathbf{q}}{\partial t} + \frac{\partial \mathbf{A_r q}}{\partial x_r} + \mathbf{C q} + \frac{\partial}{\partial x_r}\left(\frac{\partial \mathbf{C_{rs} q}}{\partial x_s}\right) = \mathbf{0} \tag{2}$$

with $\mathbf{q} = \{\tilde{\rho}, \bar{\rho}\tilde{u}_x, \bar{\rho}\tilde{u}_y\}^T$ the vector of unknown harmonic perturbations in density and conservative velocity components. The standard double decomposed LNS equations assume that the acoustic field is not directly interacting with the turbulent mixing but rather represent the turbulence contribution on the propagation of the acoustic waves solely through the turbulent mean flow quantities. It corresponds to the quasi-laminar model for the perturbation Reynolds stress, where this quantity is set to zero. Previous studies have shown that this model is accurate enough at sufficiently high frequency but underestimates the effective acoustic damping at lower frequencies [1, 3].

2.2 Triple decomposed LNS equations

In order to model the interaction between the turbulent flow perturbations and the coherent scale, a triple decomposition of the instantaneous variables can be performed, as introduced by Reynolds

and Hussain [4], which adds an extra term $\partial\left(\bar{\rho}\left(\langle u_s' u_r'\rangle - \overline{u_s' u_r'}\right)\right)/\partial x_r$ to the momentum equations compared to Eq. (1). The quantity $\tilde{\tau}_{sr}^R = \langle u_s' u_r'\rangle - \overline{u_s' u_r'} = \widetilde{u_s' u_r'}$, called the perturbation Reynolds stress, can be interpreted as the oscillation of the background Reynolds stress introduced by the passing coherent wave. This constitutes a well-known closure problem, which requires the modeling of this quantity in terms of the harmonic perturbations to get a closed set of equations. The model used in the present work is referred to as quasi-static turbulent model or also Newtonian eddy model [3, 4, 5], based on the Boussinesq turbulent viscosity hypothesis, as in [1, 6]. This assumes that the transfer of momentum caused by turbulent eddies is modeled with an effective eddy viscosity μ_t in a similar way as the momentum transfer caused by molecular diffusion. In this framework, the following relation is used:

$$\tilde{\tau}_{sr}^R = -\frac{\mu_t}{\bar{\rho}}\left(\frac{\partial \tilde{u}_s}{\partial x_r} + \frac{\partial \tilde{u}_r}{\partial x_s} - \frac{2}{3}\frac{\partial \tilde{u}_k}{\partial x_k}\delta_{sr}\right) \tag{3}$$

The way turbulence-sound interaction is accounted for in this version of the LNS equations is therefore by adding an extra damping effect through the eddy viscosity diffusive terms. With the previous expression for the perturbation Reynolds stress the equations set can be written in the same matrix formulation as Eq. (2) where only the Jacobian flux matrices $\mathbf{A_r}$ and the matrices related to the diffusive terms $\mathbf{C_{rs}}$ are modified.

3. Finite element strategy

The matrix formulation Eq. (2) for both quasi-laminar and turbulent LNS set of equations is solved using a high-order FEM (p-FEM) frequency domain solver. A set of Lobatto shape functions [7] is used here for the expansion of each field variable. The harmonic perturbation quantities are assumed to be harmonic time dependent variables that can be written as $\tilde{q}(\mathbf{x}, t) = \hat{q}(\mathbf{x})\mathrm{e}^{+\mathrm{j}\omega t}$, where $\hat{q}$ is a complex quantity and ω is the angular frequency.

All walls of the physical domain are assumed impermeable and acoustically rigid. One can apply wall slip boundary conditions ($\mathbf{u}'.\mathbf{n} = 0$) where the acoustic boundary layer is expected to play no significant role and no-slip wall boundary condition otherwise ($\tilde{\mathbf{u}} = \mathbf{0}$). Non-reflecting boundary conditions are applied on the truncated boundaries of the domain in order to avoid outgoing waves to be artificially reflected back inside the physical domain. The approach adopted in this work is the Perfectly Matched Layer (PML) technique. The stretching function and parameters used for the time/space change of coordinates introduced by the PML approach have been chosen according to [8, 9, 10].

Following the work of Hamiche [11] on the standard Petrov-Galerkin stabilization approaches applied to the Linearized Euler Equations (LEE) operator for p-FEM computations, it has been observed that the standard Galerkin/ Least-Squares (GLS) stabilization scheme allows to improve considerately the accuracy of LNS equations computations as well [12, 13] and is applied here.

4. Sound-turbulence interaction at orifice with bias flow

4.1 Description of the orifice setup

This work focuses on the acoustic scattering of a plane wave impinging on an orifice plate with a single hole with flow passing through. The computational domain for both Computational Fluid Dynamics (CFD) and acoustics is depicted in Fig. 1. The physical dimensions of the setup are $L_0 = 0.004\,\mathrm{m} \times w_0 = 0.02\,\mathrm{m}$ for the perforation and $L = 33.2\,w_0 \times H = 2\,w_0$ for the duct. The PML domains for injection of the acoustic modes into the physical domain and non-reflective boundary conditions have a length $L_{\mathrm{PML}} = 0.5\,w_0$. Boundary conditions for the CFD and LNS models are indicated as well in Fig. 1. Black lines indicate slip wall boundary condition and blue lines refer to no-slip boundary conditions, for both flow and acoustic simulations. Prescribing slip wall boundary

conditions for the duct allows one to disregard the development of the boundary layer inside the duct but still implies that the plate orifice cell behaves independently from the neighboring ones. The red color refers to the CFD domain boundaries definition applied for the incompressible Reynolds Averaged Navier-Stokes simulations. They consist in a $V_{\text{in}} = 13.6\,\text{m s}^{-1}$ velocity inlet (dotted line) corresponding to a Mach number $M = 0.0396$, pressure outlet with gauge pressure of $0\,\text{Pa}$ (dashed line), slip boundary condition for the duct walls and no-slip boundary condition for the orifice plate.

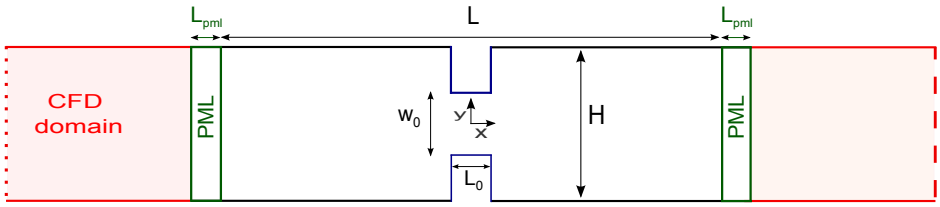

Figure 1: Overview of the 2-D plate orifice geometry

4.2 Discussion on flow results

The first step in the followed aero-acoustic hybrid methodology is to get the base flow in which the injected acoustic wave propagates. The base flow field is computed using a steady RANS simulation, carried out with the commercial CFD software ANSYS Fluent. The K-ϵ model combined with enhanced wall functions is solved using the SIMPLE algorithm. The solution of the RANS simulation is mapped onto the coarser acoustic grid, applying linear interpolation of the flow field variables and their derivatives. The flow parameters selected for the CFD simulations are the following: ratio of specific heats $\gamma = 1.4$, operating pressure $p_0 = 101\,325\,\text{Pa}$, density $\bar{\rho} = 1.205\,\text{kg m}^{-3}$ and dynamic fluid viscosity $\mu = 1.8208 \times 10^{-5}\,\text{kg m}^{-1}\,\text{s}^{-1}$.

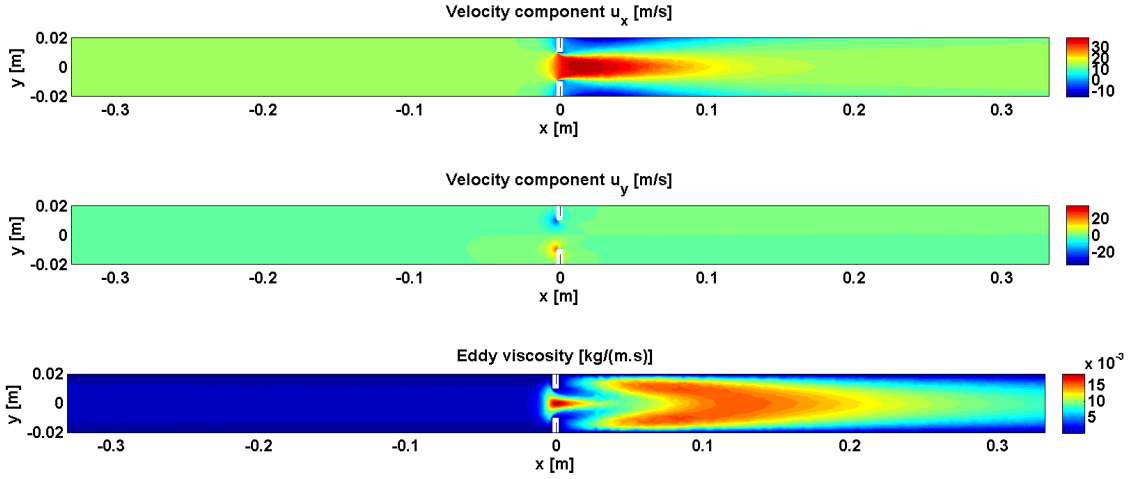

Figure 2: Based flow description from K-ϵ RANS simulation (mapped on the acoustic mesh) - $\bar{u}_x$ (top), $\bar{u}_y$ (center), μ_t (bottom).

With the inflow Mach number $M = 0.0396$, which corresponds to a duct height based Reynolds number $Re = 3.6 \times 10^4$, the maximum magnitude of the velocity in the domain is $|\bar{\mathbf{u}}| = 38.4\,\text{m s}^{-1}$, i.e. $M = 0.11$, and is obtained in the region of the orifice by the formation of a jet, which expands downstream of the perforation. Typical recirculation areas can be seen in Fig. 2 downstream of the orifice and in the orifice itself. Note that simulations with Shear Stress Transport (SST) K-ω model have been run as well, and that those recirculation areas and the spatial distribution of the eddy viscosity have shown dependency on the choice of RANS model.

4.3 Sound-turbulence interaction at orifice with bias flow

The p-FEM simulations of the coherent fields have been performed on a 2-D computational mesh with approximately 37 000 triangular linear elements and 3^{th}-order interpolating Lobatto polynomial functions, yielding a system of about 487000 degrees of freedom. The size of the smallest element is determined from the Acoustic Boundary Layer (ABL) thickness δ_a defined in a medium at rest as $\delta_a = \sqrt{2\nu/\omega}$. The value taken corresponds to $\delta_{a,min} = \delta_a(f = 5000\,\text{Hz}) = 3.1015 \times 10^{-5}\,\text{m}$, higher limit of the chosen frequency range [200 - 5000] Hz. The frequency step is 200 Hz. The mesh elements h inside the orifice are of the size $\delta_{a,min}$, whereas the element size is growing outside the duct linearly up to $h = 0.005\,\text{m}$ at $x = \pm 0.02\,\text{m}$ and further away is constant.

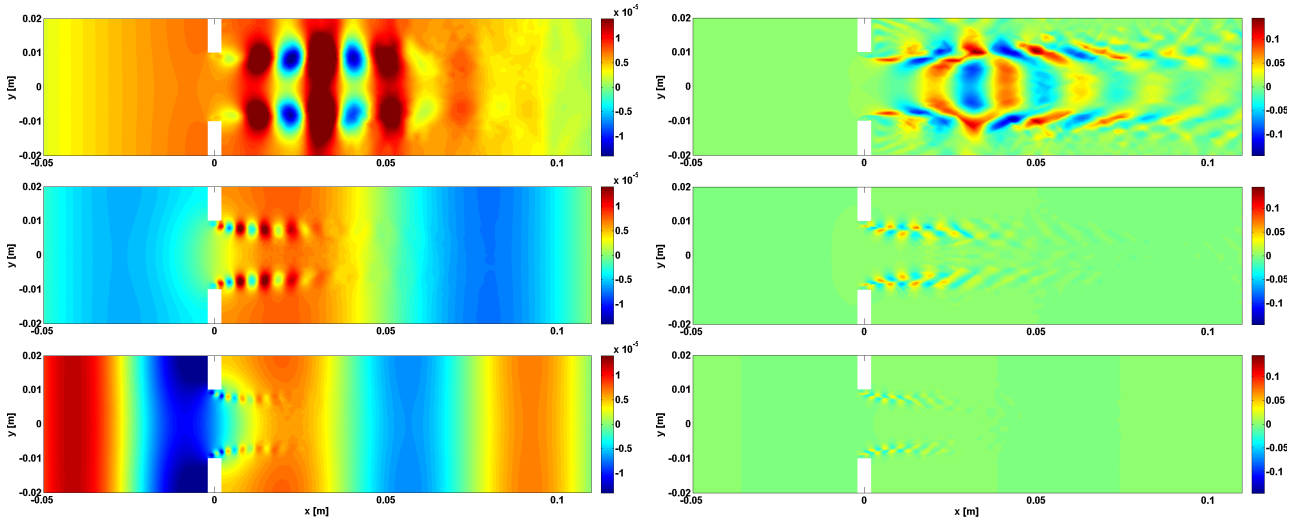

Figure 3: Quasi-laminar LNS results for the real part of the density $\tilde{\rho}$ (left, in kg m^{-3}) and velocity component $\bar{\rho}\tilde{u}_x$ (right, in kg m^{-2} s^{-1}) perturbations at $St = 0.104$ (top), $St = 0.313$ (center), $St = 0.521$ (bottom).

The coherent fields of the density $\tilde{\rho}$ and velocity component $\tilde{u}_x$ are shown in Fig. 3 at three different frequencies. The selected dimensionless frequencies $St = 0.104$, $St = 0.3125$ and $St = 0.521$ cover the range of frequencies in this study. Strouhal number values are based on the orifice thickness L_o and the orifice flow speed by $St = f\,L_o/\left|\mathbf{u}_{\mathbf{orifice}}\right|$. The perturbed field consists of both acoustic and vortical contributions. The propagating acoustic plane wave can clearly be identified with its related acoustic wavelength $\lambda_a = (1 + M)\,\bar{c}/f$, where f is the frequency and $\bar{c}$ the speed of sound. The hydrodynamic modes originating from the sound-flow interaction near the orifice edges are characterized by their shorter hydrodynamic wavelength $\lambda_h = |\bar{u}|\,/f$. The structures of the hydrodynamic modes observed in this study strongly depend on the Strouhal number St. Those modes propagates rather far from the orifice section at lower frequency, and are still significant in magnitude after several duct diameters distance. They can therefore pollute acoustic two-port measurements performed with microphones in this region. At low Strouhal numbers, the maximum of vortices magnitude is higher than at higher St. Over a low frequency range (estimated [600 - 1200] Hz) additional hydrodynamic modes can also propagate through the large recirculation areas downstream of the orifice. Results obtained with quasi-laminar LNS equations depicted in Fig. 3 show similar phenomena as found in a previous study [2], even if they cannot be quantitatively compared because of the differences in the flow and the dimensions.

Figure 4 shows the density perturbation $\tilde{\rho}$ obtained from quasi-laminar (top) and turbulent (bottom) LNS simulations with two different turbulence RANS models. The choice of the RANS model affects the predicted harmonic perturbations through the base flow properties (see quasi-laminar results) but also through the eddy viscosity. In both turbulent cases, the extra damping from the eddy viscosity decreases the amplitude of the vortical structures appearing at the orifice edges. The K-ϵ

model gives higher values of eddy viscosity inside the orifice than the SST K-ω model, which leads to an increased impact of the turbulence on the vortices. The effect on the acoustic field itself has to be further quantified.

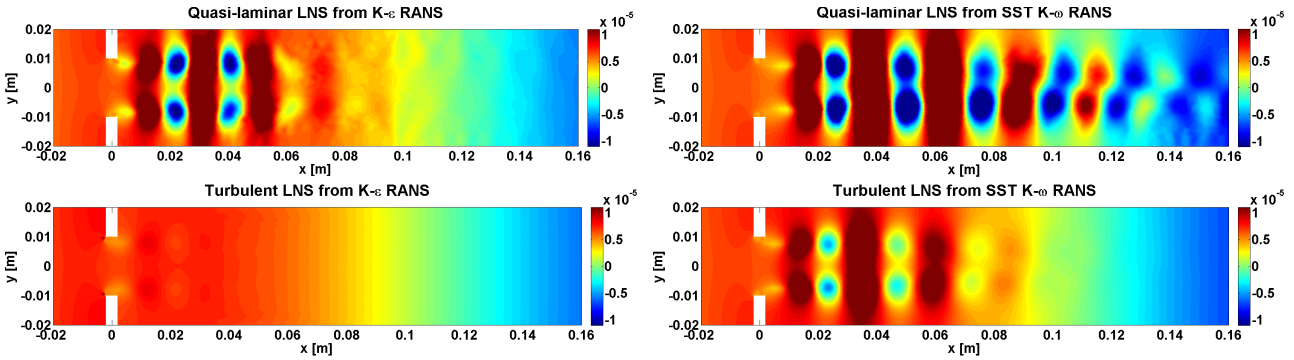

Figure 4: Effect of RANS base flow choice on LNS results for the real part of the density perturbation $\tilde{\rho}$ (kg m^{-3}) at $St = 0.104$ (i.e. $f = 1000$ Hz).

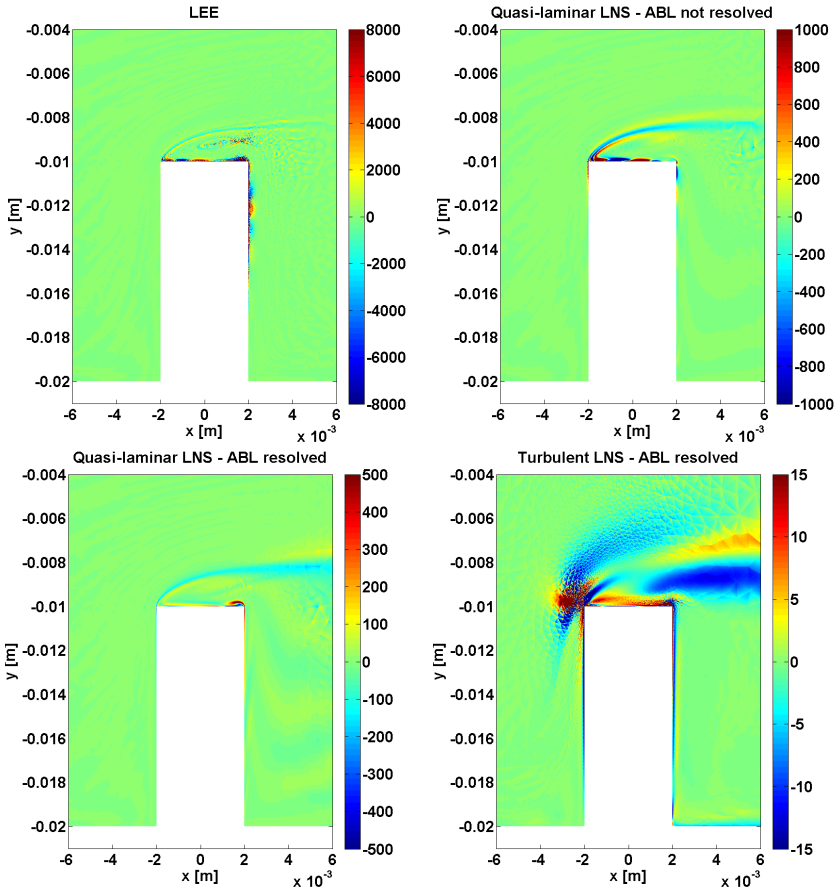

Figure 5: Vorticity field $\mathrm{Re}(\tilde{\omega})$ (s^{-1}) at $St = 0.104$ (i.e. $f = 1000$ Hz) for the 4 physical models.

Figure 5 shows the real part of the vorticity perturbations, defined as $\tilde{\omega} = \partial\tilde{u}_y/\partial x - \partial\tilde{u}_x/\partial y$, in the direct vicinity of the orifice down part for four different physical models at frequency $St = 0.104$: LEE, quasi-laminar LNSE with slip boundary condition (without resolving the ABL), quasi-laminar LNSE with no-slip boundary condition and resolving the ABL, and turbulent LNS with no-slip boundary resolving the ABL (with K-ϵ model). The same acoustic mesh is used in all cases, with mesh size $\delta_{a,min}$ inside the duct. This represents around three elements inside the ABL at the frequency $St = 0.104$.

Vorticity is shed at the leading edge and is convected along the base flow streamlines. The choice of the physical model plays an important role on the local representation of the interactions between acoustic and hydrodynamic modes in the orifice region. The addition of no-slip condition prevents the appearance of spurious modes inside the ABL and an acoustic boundary layer is formed at the orifice plate wall. The addition of fluid and eddy viscosity reduces the amplitude of the vorticity but the edges have still the dominant impact on the vorticity. The representation scale in Fig. 5 has been adapted for each case, as amplitudes of the vorticity real part change up to two orders the more diffusion is added to the model, with LEE showing the highest values. Note that the computation of the vorticity field is performed element by element and therefore one can notice discontinuities between elements when their size is large enough. From the simulations results, it can be observed that not only a refinement of the acoustic mesh is needed in the orifice region but also in the area of strong base flow gradients caused by the orifice shear. If asymmetries in the harmonic field appear at the orifice edges, such refinement however tends to amplify the asymmetric behavior of the downstream results. This behavior was not observed in reference [2] with reported mesh, where mesh size growth rate was significant also in the downstream area. The local refinement of the mesh inside the orifice improves the accuracy of the computed perturbations since it captures better the complex sound-flow interactions localized in the acoustic and turbulent boundary layers. If this area is not refined enough, the error generated inside the orifice can propagate downstream in the shear region.

5. Discussion and conclusion

This paper has presented the results of the simulation of the acoustic propagation through a plate orifice in presence of a bias flow, at low Mach Number (M=0.0396). For this purpose, a hybrid approach was applied, combining RANS steady base flow simulations and linearized acoustic operators used to compute the harmonic perturbations. Different physical models for the flow-sound interaction have been implemented in a frequency domain high-order continuous Finite Element Method solver and those models were compared on the orifice plate configuration. This study compares results coming from the isentropic version of the Linearized Euler, standard Linearized Navier-Stokes and turbulent Linearized Navier-Stokes equations.

The presented results constitute the first step in the study of sound-turbulence interaction for an orifice with bias flow. A detailed description of the coherent perturbations due to the acoustic excitation of the orifice has been given. In the quasi-laminar assumption, the vortex growth is limited solely by the fluid viscosity. In case of turbulent LNS equations, the vortical structures due to interaction of acoustic and vorticity modes are damped by the extra terms coming from the added eddy viscosity. From the present study, one can see that the extra diffusive terms linked to the effect of the flow turbulence on the coherent perturbation predominantly affect the vortices propagating downstream in the vicinity of the orifice. Nevertheless, looking at the changes in the global perturbation fields due to the added viscosity, an impact on the global acoustic behavior can be expected. This has to be further assessed, e.g. by scattering matrix representation. It has been noticed that the choice of RANS models for the base flow simulation impacts considerably the spatial distribution of eddy viscosity and affects significantly the local coherent modes. The turbulence model used for the description of the perturbation Reynolds stress $\tilde{\tau}_{ij}$ in this study is the Newtonian eddy model. Such model has already shown some limitations at sufficiently low frequencies in previous studies on duct acoustic with turbulent low Mach number flows. Alternatives, like the frequency dependent eddy-viscosity models and non-equilibrium models of the turbulent diffusion, could be implemented in the frame of the present p-FEM LNS equations solver to study their impact on the results. Future work will investigate the impact of these turbulence effects on the acoustic impedance and a possible extension of existing impedance models for orifices.

ACKNOWLEDGEMENTS

The presented work is part of the Marie Curie Initial Training Network Thermo-acoustic and aero-acoustic nonlinearities in green combustors with orifice structures (TANGO). We gratefully acknowledge the financial support from the European Commission under call FP7-PEOPLE-ITN-2012.

REFERENCES

1. Gikadi, J., Föller, S., Sattelmayer, T., Impact of Turbulence on the Prediction of Linear Aeroacoustic Interactions: Acoustic Response of a Turbulent Shear Layer, *Journal of Sound and Vibration*, **333**, 6548–6559, (2013).

2. Kierkegaard, A., Allam, S., Efraimsson, G., Abom, M., Simulations of Whistling and the Whistling Potentiality of an In-duct Orifice with Linear Aeroacoustics, *Journal of Sound and Vibration*, **331** (5), 1084–1096, (2012).

3. Weng, C., Boij, S., Hanifi, A., The Attenuation of Sound by Turbulence in Internal Flows, *Journal of the Acoustical Society of America*, **133** (6), 3764–3776, (2013).

4. Reynolds, W.C., Hussain, A.K.M.F., The Mechanics of an Organized Wave in Turbulent Shear Flow. Part 3. Theoretical Models and Comparison with Experiments, *Journal of Fluid Mechanics*, **54**, 263–288, (1972).

5. Pope, S.B., A More General Effective-viscosity Hypothesis, *Journal of Fluid Mechanics*, **72**, 331–340, (1975).

6. Holmberg, A., Kierkegaard, A., Weng, C., A Linearized Navier-Stokes Method Including Turbulence Damping, *19th AIAA/CEAS Aeroacoustics Conference*, Berlin, (2013).

7. Šolín, P., Segeth, K., Doležel , I., *Higher-Order Finite Element Methods*, CHAPMAN & HALL/CRC, 1–388, (2004).

8. Hamiche, K., Gabard, G., Beriot, H., A Higher-Order Finite Element Method for the Linearised Euler Equations, *In Proceedings of the International Conference on Noise and Vibration Engineering ISMA 2014*, Leuven, Belgium, 1311–1325 (2014).

9. Bécache, E., Bonnet-Ben Dhia, A.S., Legendre, G., Perfectly Matched Layers for the Convected Helmholtz Equation, *SIAM J. Numer. Anal.*, **42** (1), 409–433, (2004).

10. Bermùdez, A., Hervella-Nieto, L., Prieto, A., Rodríguez, R., An Optimal Perfectly Matched Layer With Unbounded Absorbing Function for Time-harmonic Acoustic Scattering Problems, *Journal of Computational Physics*, **223**, 469–488, (2007).

11. Hamiche, K., Beriot, H., Gabard, G., Application of a High-Order FEM Solver to Aeroengine Exhaust Noise Radiation, *EuroNoise 2015*, Maastricht, The Netherlands, (2015).

12. Gikadi, J., Schulze, M., Schwing, J., Föller, S., Sattelmayer, T., Linearized Navier-Stokes and Euler Equations for the Determination of the Acoustic Scattering Behaviour of an Area Expansion, *18th AIAA/CEAS Aeroacoustics Conference*, **AIAA2012-2292**, Colorado Springs, CO, (2012).

13. Rao, P., Morris, P.J., Use of Finite Element Methods in Frequency Domain aeroacoustics, *AIAA Journal*, **44**, 1643–1652, (2006).